

Formation of Heavy Meson Bound States by Two Nucleon Pick-up Reactions

N. Ikeno,¹ J. Yamagata-Sekihara,^{2,3} H. Nagahiro,¹ D. Jido,³ and S. Hirenzaki¹

¹*Department of Physics, Nara Woman's University, Nara 630-8506, Japan*

²*Departamento de Física Teórica and IFIC, Centro Mixto Universidad de Valencia-CSIC, Institutos de Investigación de Paterna, Aptdo. 22085, 46071 Valencia, Spain*

³*Yukawa Institute for Theoretical Physics, Kyoto University, Kyoto 606-8502, Japan*

(Dated: November 1, 2011)

We develop a model to evaluate the formation rate of the heavy mesic nuclei in the two nucleon pick-up reactions, and apply it to the ${}^6\text{Li}$ target cases for the formation of heavy meson- α bound states, as examples. The existence of the quasi-deuteron in the target nucleus is assumed in this model. It is found that the mesic nuclei formation in the recoilless kinematics is possible even for heavier mesons than nucleon in the two nucleon pick-up reactions. We find the formation rate of the meson- α bound states can be around half of the elementary cross sections at the recoilless kinematics with small distortions.

PACS numbers: 21.85.+d, 36.10.Gv, 25.10.+s

I. INTRODUCTION

Meson-Nucleus systems are one of the most interesting laboratories to study the meson properties at finite density and to explore the symmetry breaking pattern of QCD and its partial restoration in nucleus [1–3]. Especially, the studies of the bound states of meson and nucleus have the following advantages; (i) the selective observation of the meson properties is possible by making use of the fixed quantum numbers of the bound states, (ii) the meson properties inside the nucleus can be observed clearly only with relatively small contamination from the vacuum processes, and (iii) the system is quasi-static and the time dependent dynamical evolution of the system is irrelevant. These features are different from other methods based on the scattering and collision processes. On the other hand, the information obtained from the observation of the bound states are limited in $\rho \lesssim \rho_0$ and $T = 0$ region in the QCD phase diagram.

We have studied so far the physical interests, the structures, and the formation reactions of the various kinds of the meson-nucleus systems [4–6]. Within these studies, the most exciting and successful results were obtained by the observation of deeply bound pionic atoms in the one nucleon pick-up ($d, {}^3\text{He}$) reactions [2, 4, 7]. We have also considered other one nucleon pick-up reactions like (γ, p) [8] and (π, N) [9] for the mesic nuclei formations. The one nucleon pick-up reactions are found to be useful for the mesic nucleus formation, however, they require the large momentum transfer for heavy meson production which is one of the main obstacle to observe bound states. Thus, we think that we need to develop new methods for bound state formations to extend our studies to other meson-nucleus systems, especially for heavier mesons. Actually, we are interested in the heavy meson-nucleus systems such as $\eta'(958)$ meson for the studies of $U_A(1)$ anomaly effects [10–12], ϕ meson for $\bar{s}s$ components of nucleon and OZI rule at finite density [13], and D mesons for the charm meson properties in nucleus [14]. Thus, we would like to study the two nucleon pick-up re-

actions theoretically as a possible method suited to form the heavy meson nucleus bound systems.

One of the most serious problems in the formation reactions of the heavy meson nucleus systems are the large momentum transfer as mentioned above. It is known that the matching condition of momentum and angular momentum transfers plays an important role to determine the largely populated subcomponents and it is also known that the best choice for our purpose is the total angular momentum transfer $J = 0$ state formation in the recoilless kinematics in many cases. In the one nucleon pick-up reactions which we have mainly considered so far, the recoilless kinematics can not be satisfied for the formation of heavier meson bound states than the nucleon mass because of the large mass of the meson. Thus, we consider the two nucleon pick-up reactions in this article to investigate the possibility to extend our study to heavier meson region using these reactions. Actually, there was an attempt to observe the η -mesic state in the two nucleon pick-up ${}^{27}\text{Al}(p, {}^3\text{He})$ reaction at COSY-GEM [15].

II. EFFECTIVE NUMBER FORMALISM FOR THE QUASI-DEUTERON IN NUCLEUS

We formulate the formation cross section of the heavy meson bound states by the two nucleon pick-up reactions. As we will see below, our model is so simple that it can be applied generally to the heavy meson bound state formations by the two nucleon pick-up reactions such as (γ, d) and $(p, {}^3\text{He})$.

We apply the effective number approach, which has been used for the studies of the meson-nucleus bound states [4], to evaluate the formation rate of the bound systems in the two nucleon pick-up reactions. In the effective number approach, the formation cross section

by the two nucleon pick-up reactions can be written as,

$$\frac{d^2\sigma}{dEd\Omega} = \left(\frac{d\sigma}{d\Omega}\right)^{\text{ele}} \sum_f \frac{\Gamma}{2\pi} \frac{1}{\Delta E^2 + \Gamma^2/4} N_{\text{eff}}, \quad (1)$$

where $(d\sigma/d\Omega)^{\text{ele}}$ is the elementary cross section of the meson production, and Γ the width of the meson bound states. The all combinations of the final states, labeled by f , are summed up to evaluate the inclusive cross section. The energy transfer ΔE of the reaction in the laboratory frame is defined as,

$$\Delta E = (T_f + M_f) + (M - B) - (T_i + M_i) - (2M_N - S_{2N}), \quad (2)$$

where T_f and M_f are the kinetic energy and the mass of the emitted particle, T_i and M_i the kinetic energy and the mass of the incident particle, and M the mass of the produced meson. The meson binding energy B and the two nucleon separation energy S_{2N} from the target nucleus are determined for each bound level of meson and excited level of the daughter nucleus. Here, we neglect the recoil energy of the nucleus.

The momentum transfer \mathbf{q} of the reaction is defined as,

$$\mathbf{q} = \mathbf{p}_i - \mathbf{p}_f, \quad (3)$$

and shown in Fig. 1 for the ϕ meson formation case, as an example, in the heavy target for the (γ, d) reaction together with that for one-nucleon pick-up (γ, N) reaction as functions of the momentum of the incident photon. We also show the momentum transfers for the $(p, {}^3\text{He})$ and (p, d) reactions for the ϕ meson formation in Fig. 2 for comparison. As we can see from the figures, the two-nucleon pick-up reactions satisfy the recoilless condition $\mathbf{q} = 0$ at a finite incident momentum, while large momentum transfer is unavoidable for the one-nucleon pick-up reactions. We show in Fig. 3 the incident beam momenta p for the four reactions required to produce the meson with an effective mass M^* in recoilless kinematics. The effective mass M^* is defined as $M^* = M - B$ with the meson mass M and the binding energy B . We find clearly that the meson with larger effective mass than nucleon can not be produced in recoilless kinematics by the one nucleon pick-up reactions. In two nucleon pick-up reactions like (γ, d) and $(p, {}^3\text{He})$, on the other hand, we can produce the heavier meson states like $\eta'(958)$, $\phi(1020)$, and $a_1(1260)$ meson bound states in the recoilless kinematics.

The theoretical calculation of the two nucleon pick-up reactions is rather difficult in general. In addition, we expect complicated nuclear excitations in daughter nuclei with two nucleon holes, which will prevent us from the clear identification of meson bound states. Here, we consider the specific nucleus ${}^6\text{Li}$ as the target which has the well-developed cluster structure of $\alpha + d$ in the ground state. The probability of the $\alpha + d$ component of the ground state of ${}^6\text{Li}$ is reported to be 0.616 in Ref. [16] and 0.73 in Ref. [17]. In the reaction considered in this

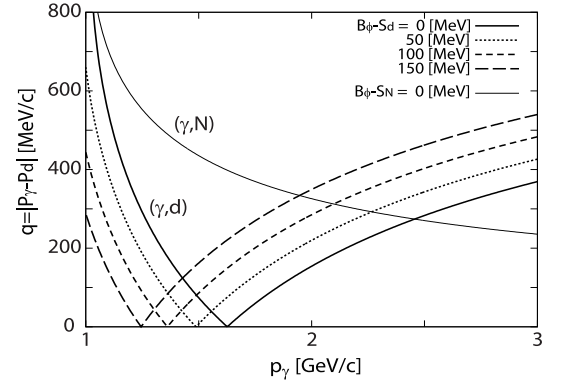


FIG. 1. Momentum transfer \mathbf{q} of the forward (γ, d) reaction for the formation of $\phi(1020)$ meson bound states in the heavy target nucleus plotted as functions of the incident photon momentum p_γ for four values of the gap $(B_\phi - S_d)$ between the ϕ meson binding energy B_ϕ and the deuteron separation energy S_d as indicated in the figure. Momentum transfer of the one-nucleon pick-up (γ, N) reaction is also shown for comparison.

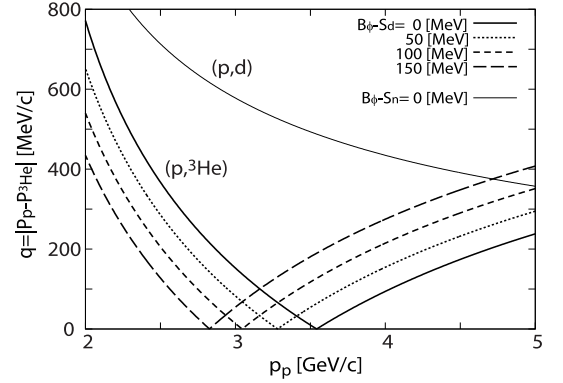


FIG. 2. Same as Fig. 1 except for the proton induced $(p, {}^3\text{He})$ and (p, d) reactions.

article, the momentum transfer to the initial deuteron wavefunction in ${}^6\text{Li}$ and the final meson wavefunction in the mesic nucleus is considered to be small near the recoilless kinematics and the quasi-deuteron picture in the ${}^6\text{Li}$ target is expected to be a good approximation. Thus, by considering the nuclei like ${}^6\text{Li}$ which have the large component of quasi-deuteron as targets, we can evaluate the reaction rate in a simple way and expect to have the simple structure of the formation spectra of mesic nuclei in the two nucleon pick-up reactions. In our model considered, we treat ${}^6\text{Li}$ as the bound state of the alpha particle and the deuteron to evaluate the reaction rate. Thus, B in Eq. (2) is the binding energy of a heavy meson and α particle in the final state and S_{2N} is fixed to be $S_{2N} = 1.47$ [MeV] from the mass gap of initial and final nuclei as $S_{2N} = (M_\alpha + M_d) - M_{{}^6\text{Li}}$. The elementary cross section $(d\sigma/d\Omega)^{\text{ele}}$ for the meson production appearing in Eq. (1) is that of the $i + d \rightarrow f + \text{meson}$

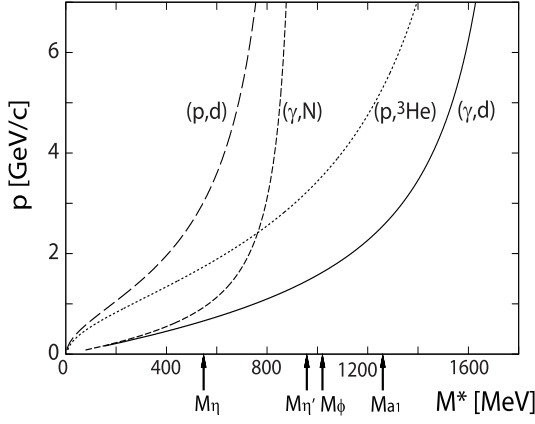


FIG. 3. Incident beam momenta p required to produce meson in recoilless kinematics in one nucleon pick-up $((\gamma, N), (p, d))$ and two nucleon pick-up $((\gamma, d), (p, {}^3\text{He}))$ reactions are plotted as functions of meson effective mass M^* which is defined as $M^* = M - B$ with the meson mass M and the binding energy B . The in-vacuum masses of η , η' , ϕ and a_1 are indicated in the figure by arrows.

reaction with the incident particle i and the emitted particle f , which should be evaluated from experiments as previous cases [4–6]. Here, the emitted particle f will be ${}^3\text{He}$ for the proton induced ($i = \text{proton}$) case, and d for the γ induced ($i = \text{photon}$) case, respectively.

In our model considering the ${}^6\text{Li}$ nucleus as the bound state of alpha particle and deuteron, the effective number N_{eff} of the ${}^6\text{Li}(i, f)\alpha \otimes \text{meson}$ reaction can be written as,

$$N_{\text{eff}} = \sum_{JM} \left| \int \chi_f^*(\mathbf{r}) [\phi_{l_m}^*(\mathbf{r}) \otimes \psi_{l_d}(\mathbf{r})]_{JM} \chi_i(\mathbf{r}) d\mathbf{r} \right|^2, \quad (4)$$

where $\phi_{l_m}(\mathbf{r})$ is the wavefunction of the meson bound state and $\psi_{l_d}(\mathbf{r})$ that of the deuteron bound to α in the ${}^6\text{Li}$ target. $\chi_i(\mathbf{r})$ and $\chi_f(\mathbf{r})$ are the incident and the emitted particle wavefunctions in the scattering states, respectively. We assume plane waves for χ_i and χ_f in this article. The distortion effects to χ_i and χ_f depend on the incident and emitted particles [8], however they are known to be relatively small for the cases satisfying the matching condition [4]. The deuteron wavefunction ψ_{l_d} in ${}^6\text{Li}$ is determined to reproduce the momentum distribution reported in Ref. [17] based on the analysis of the ${}^6\text{Li}(e, e'd){}^4\text{He}$ reaction. We calculate the ψ_{l_d} by solving the Schrödinger equation with the Woods-Saxon type potential,

$$U(r) = \frac{U_0}{1 + \exp[(r - R)/a]}, \quad (5)$$

and adjust the potential depth U_0 and the radius parameter R to reproduce the momentum distribution $\rho(p)$ reported in Ref. [17]. $\rho(p)$ is defined as,

$$\rho(p) = \frac{1}{(2\pi)^3} \left| \int e^{-i\mathbf{p}\cdot\mathbf{r}} \psi_{l_d}(\mathbf{r}) d\mathbf{r} \right|^2, \quad (6)$$

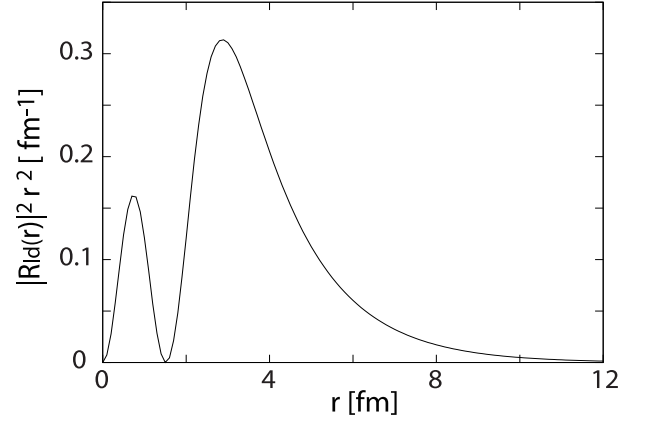


FIG. 4. Calculated density distribution of the radial part $R_{l_d}(r)$ of the relative wavefunction $\psi_{l_d}(\mathbf{r})$ of α and deuteron in ${}^6\text{Li}$ nucleus.

where $|\psi_{l_d}(\mathbf{r})|^2$ is normalized to be 1 in the coordinate space as usual. The potential parameters used here are fixed to be $R = 2.0$ [fm], $a = 0.5$ [fm], and $U_0 = -75$ [MeV]. The calculated wavefunction is shown in Fig 4 and momentum distribution in Fig. 5. The wavefunction in Fig. 4 corresponds to the $2s$ bound state as indicated in Ref. [17] because of the Pauli effect to nucleons which forbids the alpha and deuteron clusters to be in the relative $1s$ state. The calculated momentum distribution reproduce the PWIA result in Ref. [17] reasonably well as shown in the Fig. 5. In Fig. 5, we multiply a factor 0.73 to our results to correct the overall normalization of $\rho(p)$ to be the same as Ref. [17]. It should be noted that the PWIA results in Ref. [17] ignoring the distortion effects are the quantity which should be compared with our results calculated by Eq. (6).

The bound meson wavefunctions $\phi_{l_m}(\mathbf{r})$ in the final state are calculated by solving the Klein-Gordon equation with the optical potential in the Woods-Saxon form as in Eq. (5). We fix the meson mass to be $M = 1020$ [MeV] as ϕ meson, which is heavier than nucleon and cannot be formed in the recoilless kinematics in one nucleon pick-up reactions. Since mesons can be absorbed by the nucleus generally, the potential strength U_0 in Eq. (5) is considered to be a complex number as $U_0 = (V_0 + iW_0)$ for mesons. In the present calculation, we consider a few potential strengths as examples and study how the two nucleon pick-up reaction spectra change according to the meson-nucleus interaction. We consider first the potential strengths based on the experimental data obtained by E325 in KEK [18], where the ϕ meson mass shift is reported as $\Delta m(\rho_0)/m = -3.4\%$ and the ϕ meson width in nucleus $\Gamma_\phi(\rho_0) = 15$ [MeV]. We adopt these numbers as the ϕ mesic optical potential and fix as $(V_0, W_0) = (-34.7, -7.5)$ [MeV]. We mention here that the large in-medium width $\Gamma_\phi(\rho_0) \simeq 80$ [MeV] of ϕ meson was also indicated based on another attenuation experiment by LEPS at SPring-8 [19], which corre-

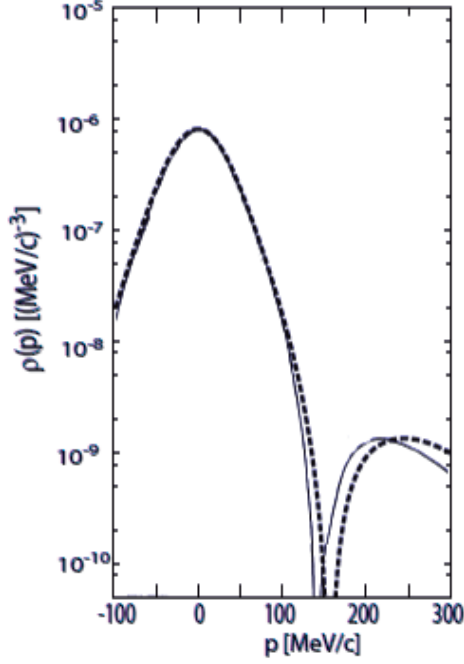


FIG. 5. Momentum distribution of deuteron in ${}^6\text{Li}$ obtained by our model (dashed line) and by the analysis of the experimental data [17] (solid line). The correction factor 0.73 is multiplied to the results of our model to satisfy the same normalization as in Ref. [17].

sponds to the imaginary potential strength $W_0 = -40$ [MeV]. We have checked numerically that the potential with this imaginary strength together with the real part strength corresponding to the 3.4 % mass reduction does not provide ϕ meson bound states in alpha potential. We, then, assume a stronger attractive potential for meson-nucleus system to estimate the formation rate of heavy meson bound systems with strong attractive potential as reported in Ref. [11] for $\eta'(958)$ meson in a theoretical model. The assumed potential parameters with two different absorption strength are $(V_0, W_0) = (-250, -5)$ and $(-250, -20)$ in unit of MeV. The distribution parameters are fixed to be $R = 1.18A^{1/3} - 0.48$ [fm] and $a = 0.5$ [fm] with $A = 4$ for meson-alpha system. We show in Table I the calculated binding energies and widths of the meson bound states for the three different potentials. The radial density distributions are also shown in Fig. 6 for $(V_0, W_0) = (-34.7, -7.5)$ and $(-250, -5)$ [MeV] cases. We found the radial density distributions of $1s$ states of the both potentials are much different because of the different potential strength.

Since the angular momentum l_d of the relative wavefunction of deuteron and α particle in ${}^6\text{Li}$ is considered to be 0, the expression of the effective numbers in Eq. (4)

TABLE I. Calculated binding energies and widths of the meson-alpha bound states in unit of MeV with the potential strength $(V_0, W_0) =$ (i) $(-34.7, -7.5)$, (ii) $(-250, -5)$, and (iii) $(-250, -20)$ [MeV]. The meson mass is fixed to be 1020 MeV.

(n_ϕ, ℓ_ϕ) state	(i)		(ii)		(iii)	
	B.E.	Γ	B.E.	Γ	B.E.	Γ
1s	0.76	2.9	131.5	8.1	131.2	32.5
2s			14.5	2.8	14.2	11.2
2p			58.0	5.5	57.7	21.8
3d			2.9	2.8	2.4	11.3

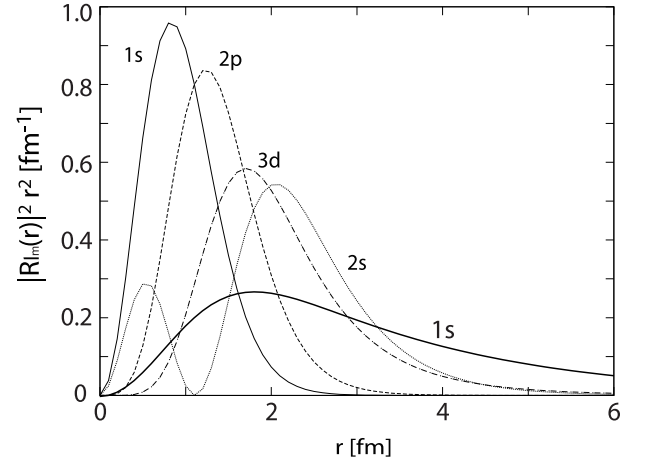


FIG. 6. Calculated density distribution of the radial part $R_{lm}(r)$ of the wavefunction $\phi_{lm}(\mathbf{r})$ of the meson bound state in the α particle for the potential strength $(V_0, W_0) = (-34.7, -7.5)$ [MeV] (thick solid line) and $(-250, -5)$ [MeV] (thin lines).

can be simplified as,

$$N_{\text{eff}} = \sum_M \left| \int e^{i\mathbf{q}\cdot\mathbf{r}} \phi_{lm}^*(\mathbf{r}) \psi_0(\mathbf{r}) d\mathbf{r} \right|^2, \quad (7)$$

in the plane wave approximation. We use this expression to calculation the effective numbers in this article.

In the recoilless kinematics, the only s states of the meson bound states can be populated because of the orthogonality of the angular part of the wavefunction as can be seen in Eq. (7). And because of the approximate orthogonality of the radial parts of ϕ_{lm} and ψ_0 , the substitutional $2s$ state of the meson is expected be largely populated.

III. NUMERICAL RESULT FOR BOUND STATE FORMATION RATE

To investigate the momentum transfer dependence of N_{eff} for each bound state formation, we show in Fig. 7

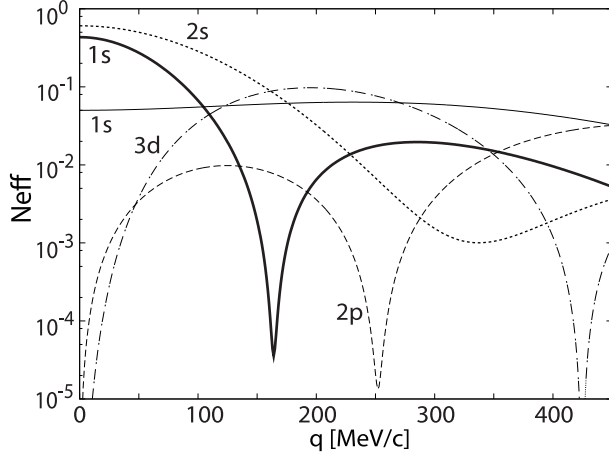


FIG. 7. Calculated effective numbers are plotted as functions of the momentum transfer of the two nucleon pick-up reactions for ${}^6\text{Li}$ target for the $1s$ meson bound state formation with the potential strength $(V_0, W_0) = (-34.7, -7.5)$ [MeV] (thick solid line) and the $1s$, $2s$, $2p$, and $3d$ bound states with $(V_0, W_0) = (-250, -5)$ [MeV] (thin lines).

the calculated effective numbers N_{eff} by Eq. (7) as functions of the momentum transfer $|\mathbf{q}|$ for two nucleon pick-up reactions for ${}^6\text{Li}$ target. Each effective number has the characteristic behavior due to the matching condition of the momentum transfer and the angular momentum transfer. As we have mentioned in the previous section, the effective numbers N_{eff} is exactly 0 for $2p$ and $3d$ states at $|\mathbf{q}| = 0$ because of the orthogonality condition of the angular part wavefunction to the s -wave function ψ_0 . And the substitutional $2s$ state of the bound meson have the largest contribution at $|\mathbf{q}| = 0$ as we expected. The contribution of the $1s$ state with weaker real potential $V_0 = -34.7$ [MeV] has the stronger dependence on q as naturally expected its larger special dimensions as shown in Fig. 6. As the momentum transfer increases, the $3d$ bound state formation has the largest contribution at $160 \lesssim |\mathbf{q}| \lesssim 270$ [MeV/c] and, then the $1s$ bound state at $270 \lesssim |\mathbf{q}| \lesssim 450$ [MeV/c]. Overall strength of the heavy meson bound state formation cross section becomes smaller for the kinematics with larger momentum transfer.

We show the same effective numbers as functions of the incident particle energies for (γ, d) and $(p, {}^3\text{He})$ reaction cases in Figs. 8 and 9. Because of the different binding energies of the meson appearing in Eq. (2), the incident particle energy which corresponds to recoilless kinematics ($|\mathbf{q}| = 0$) is different for each bound state. We indicate the incident particle energy of the recoilless kinematics for each state by the arrow in Figs. 8 and 9. The both figures show the very similar behavior of N_{eff} .

We find that the substitutional $2s$ state of the meson is produced in the almost recoilless condition and has the largest contribution to the cross section at $p_\gamma = 1.6$ [GeV/c] ($T_p = 2.7$ [GeV]). (In the explanation below,

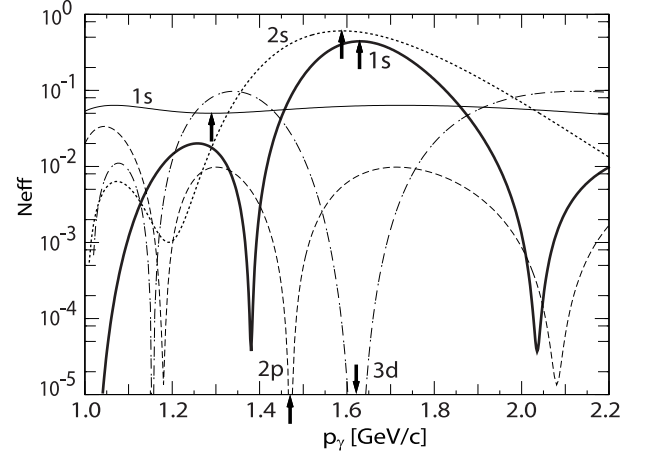


FIG. 8. Same as Fig. 7 except for the plots as functions of the incident photon momentum p_γ for (γ, d) reaction. The arrow indicates the incident photon momentum of the recoilless kinematics for each meson bound state formation.

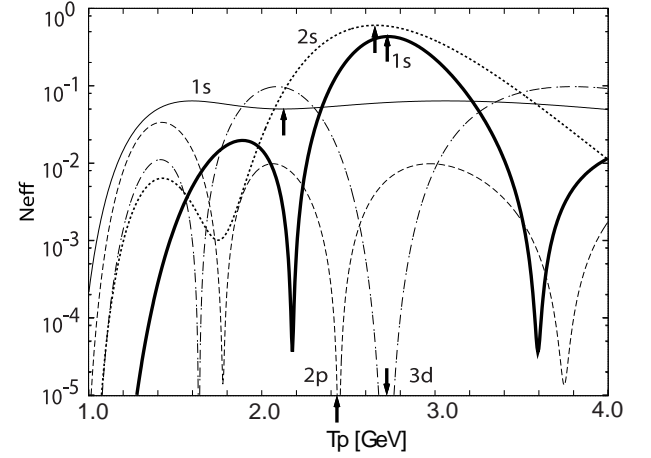


FIG. 9. Same as Fig. 7 except for the plots as functions of the incident proton kinetic energy T_p for $(p, {}^3\text{He})$ reaction. The arrow indicates the incident proton kinetic energy of the recoilless kinematics for each meson bound state formation.

we indicate the photon momentum p_γ in (γ, d) reaction with the corresponding proton kinetic energy T_p in the $(p, {}^3\text{He})$ reaction in the parenthesis.) We mention here that the $1s$ state wavefunction with the potential strength $(V_0, W_0) = (-34.7, -7.5)$ [MeV] has larger spatial dimension which violates the approximate orthogonality of the radial part with ψ_0 at $q = 0$ in Eq. (7), and thus, the contribution of this $1s$ state also has the large contribution at $p_\gamma = 1.6$ [GeV/c] ($T_p = 2.7$ [GeV]). At $p_\gamma = 1.35$ [GeV/c] ($T_p = 2.1$ [GeV]), a little above the ϕ production threshold of the elementary process, the size of the effective number of the $2s$ and $3d$ states are similar and larger than those of other states formation. At $p_\gamma = 1.8$ [GeV/c] ($T_p = 3.1$ [GeV]), the effective number of the $2s$ state formation is still dominant, however

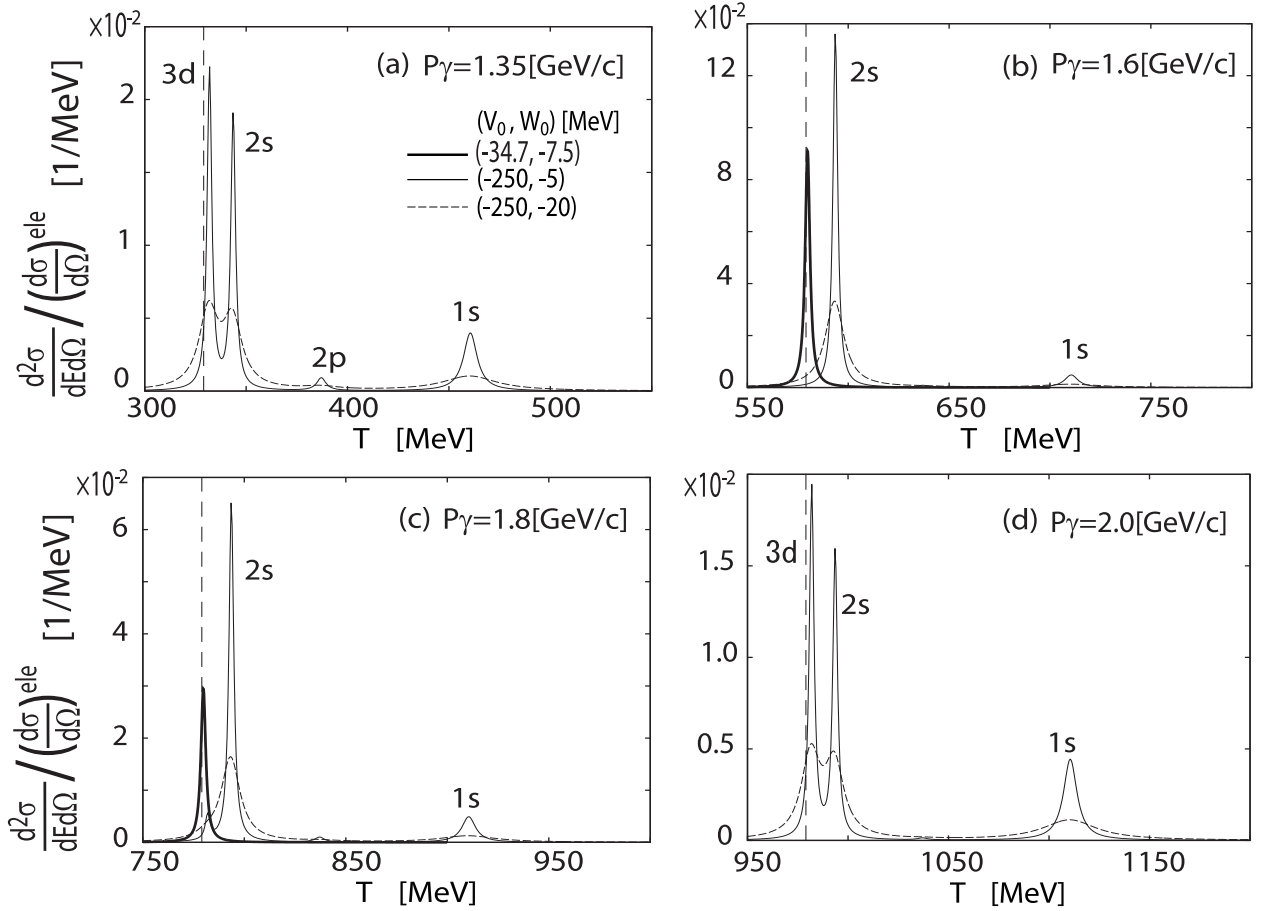


FIG. 10. Expected spectra of the forward two nucleon pick-up (γ, d) reaction ${}^6\text{Li}$ for the formation of the meson- α bound states are plotted as functions of the emitted deuteron kinetic energy for the incident photon momenta $p_\gamma =$ (a) 1.35, (b) 1.6, (c) 1.8, and (d) 2.0 [GeV/c]. The vertical dashed line indicates the meson production threshold. Each line is calculated with the different optical potential parameters for meson- α system as indicated in (a). The spectrum with the potential $(V_0, W_0) = (-34.7, 7.5)$ [MeV] is only shown in (b) and (c) because it is small and invisible in (a) and (d).

the other contributions of the $1s$ and $3d$ states formation become relatively more important than at $p_\gamma = 1.6$ [GeV/c] ($T_p = 2.7$ [GeV]). The contributions of the $1s$, $2s$, and $3d$ state formations are important at $p_\gamma = 2.0$ [GeV/c] ($T_p = 3.5$ [GeV]) and the formation spectrum is expected to be a little more complicated than those at other photon momenta. We find that N_{eff} for $2s$ bound state formation takes the largest value $N_{\text{eff}} = 0.606$ at $p_\gamma = 1.59$ [GeV/c] ($T_p = 2.66$ [GeV]) which means that the meson bound state formation cross section can be about half of the elementary cross section.

We then calculate the relative strength of the formation spectra of the meson bound states in alpha particle by the two nucleon pick-up reaction in ${}^6\text{Li}$ target at incident photon momenta $p_\gamma = 1.35, 1.6, 1.8$ and 2.0 [GeV/c] for the (γ, d) reaction which corresponds to the $T_p = 2.1, 2.7, 3.1$ and 3.5 [GeV] for the ($p, {}^3\text{He}$) reaction. We can expect to observe the different behavior of the formation spectra at these energies as expected from the energy dependence of the effective numbers. The cal-

culated results $\frac{d^2\sigma}{dE d\Omega} / \left(\frac{d\sigma}{d\Omega}\right)^{\text{ele}}$ for (γ, d) reaction are shown in Fig. 10 for three different optical parameters for the meson bound in α particle.

The expected spectra for the potential strength $(V_0, W_0) = (-34.7, -7.5)$ [MeV] case are simple since there is only lightly bound $1s$ state. As shown in Fig. 10 (b) and (c), this $1s$ state is seen as a peak close to this meson production threshold for $p_\gamma = 1.6$ and 1.8 [GeV/c] ($T_p = 2.7$ and 3.1 [GeV]). The contribution of this state has so strong q and incident energy dependence as shown in Figs. 7-9 and that it becomes smaller than those with deeper potential cases and invisible in Fig. 10 (a) and (d).

For deeper potential cases with $(V_0, W_0) = (-250, -5)$ and $(-250, -20)$ [MeV], we find that the spectra at $p_\gamma = 1.6$ and 1.8 [GeV/c] ($T_p = 2.7$ and 3.1 [GeV]) are dominated by the $2s$ state formation and the other contributions are significantly small. On the other hand, we can observe clear peak structures of the $1s$ and $3d$ states

formation in addition to the $2s$ state at $p_\gamma = 1.35$ and 2.0 [GeV/c] ($T_p = 2.1$ and 3.5 [GeV]). The size of the spectra $\frac{d^2\sigma}{dEd\Omega} / \left(\frac{d\sigma}{d\Omega}\right)^{\text{ele}}$ are relatively large at $p_\gamma = 1.6$ and 1.8 [GeV/c] ($T_p = 2.7$ and 3.1 [GeV]) where the momentum transfer of the two nucleon pick-up reactions is small. At $p_\gamma = 1.8$ and 2.0 [GeV/c] ($T_p = 3.1$ and 3.5 [GeV]), the momentum transfer is larger and the size of the spectra become smaller rapidly for the larger incident momentum and energy. We also show the effects of the imaginary part of the optical potential to the formation spectra in Fig. 10. Since we have only one deuteron state in the initial nucleus ${}^6\text{Li}$, the reaction spectra have simple structure, especially for $(V_0, W_0) = (-34.7, -7.5)$ [MeV] potential case. Thus, the main effects of the absorptive potential are found to reduce the peak height with large width. The overlap of the resonance peaks due to the widths only happens between $2s$ and $3d$ states for the absorption potential strengths studied here in the two nucleon pick-up spectra.

In case if the imaginary potential is large as $W_0 = -40$ [MeV] as indicated based on the data reported for the ϕ meson in Ref. [19], the height of all peaks in the spectra shown in Fig. 10 becomes lower in inverse proportion to the strength of the imaginary potential and the contributions of $2s$ and $3d$ states for $V_0 = -250$ [MeV] case can not be distinguished because of the large widths.

IV. SUMMARY

We have considered the two nucleon pick-up reactions in this article to investigate the feasibility of the reactions of this type to extend our research field of the meson nucleus bound systems to the heavier meson region. We have developed a model and used the effective number approach to evaluate the formation rate. As an example, we have applied the model to the heavy meson bound state formation in alpha particle with ${}^6\text{Li}$ target. As shown in the numerical results, we have found that the shape of the formation spectra is simple and seems to be suited to extract the binding energies and widths of the meson bound state because of the simple $\alpha - d$ cluster structure of ${}^6\text{Li}$. The size of the formation cross section can be more than half of the elementary cross section at the recoilless kinematics.

This theoretical model is so simple that we can apply it easily to evaluate the mesic nucleus formation rate of other two nucleon pick-up reactions such as (π, d) and so on. To do this, we should simply replace the elementary cross sections to those of the appropriate processes of the meson production like $\pi + d \rightarrow d + \text{heavy meson}$. In this model, however, the target nucleus is required to have large component of the quasi deuteron structure. Thus,

we have considered the ${}^6\text{Li}$ target as an example in this article. The calculated spectra shape are expected to have simple structure generally because of the existence of the quasi-deuteron in target nucleus and are suited to extract meson properties from the reaction spectra.

In general cases, we should not assume the existence of the quasi deuteron in the target nuclei [20] and we need to evaluate the emissions of the deuteron composed of two nucleons which are in the different single particle levels in the target. The deuteron can be formed from any pairs of proton and neutron in the target by the reaction of the meson production. In this process, however, the spectrum shape could be so complicated that it is difficult to extract meson properties.

As for the actual experimental observations, the calculated cross sections could be too small to find peak structures in the inclusive missing mass spectra due to the size of the elementary cross section, and the coincident measurement detecting the particle pair emissions from meson absorption in nucleus may be necessary to reduce the background. So far, the formation η mesic nucleus in the two nucleon pick-up $(p, {}^3\text{He})$ reaction for ${}^{27}\text{Al}$ target was reported in Ref [15] by COSY-GEM. They performed the coincidence measurement with $p\pi^-$ pair emissions from ηN in nucleus. They reported 0.5 [nb] for the upper limit of the signal of the η mesic nuclear formation cross section [15] at the energy where the elementary cross section is 77 [nb/sr] [21]. In our example considered in this article, the effective number N_{eff} for the formation of meson bound state is about 0.5 for both shallow and deep potential cases around $p_\gamma = 1.6$ [GeV/c] ($T_p = 2.7$ [GeV]) for the largest contributions as shown in Fig. 8. In this sense, we think the present result also have relevance as a guide for the actual experiment.

We believe that it is quite important to find new reactions suited to form the heavy meson bound states in nucleus to explore the various aspects of the strong interaction symmetries at finite density by the mesic nuclei. In this context, the two nucleon pick-up reactions studied in this article are quite interesting, since we can satisfy the recoilless condition in this reaction for the formation of meson heavier than nucleon.

ACKNOWLEDGMENTS

We acknowledge the fruitful discussions with H. Fujioka and K. Itahashi. N. I. appreciates the support by the Grant-in-Aid for JSPS Fellows. This work was partly supported by the Grants-in-Aid for Scientific Research (No. 22740161, No. 20540273, and No. 22105510). This work was done in part under the Yukawa International Program for Quark-hadron Sciences (YIPQS).

[1] T. Hatsuda and T. Kunihiro, Phys. Rept. **247**, 221 (1994), and references therein.

[2] D. Jido, T. Hatsuda and T. Kunihiro, Phys. Lett. **B670**,

- 109 (2008).
- [3] E. E. Kolomeitsev, N. Kaiser, and W. Weise, Phys. Rev. Lett. **90**, 092501 (2003).
 - [4] H. Toki, S. Hirenzaki, T. Yamazaki and R. S. Hayano, Nucl. Phys. **A501** (1989), 653;
S. Hirenzaki, H. Toki, and T. Yamazaki, Phys. Rev. **C44**, 2472 (1991);
H. Toki, S. Hirenzaki, and T. Yamazaki, Nucl. Phys. **A530**, 679 (1991).
 - [5] T. Kishimoto, Phys. Rev. Lett. **83**, 4701 (1999);
S. Hirenzaki, Y. Okumura, H. Toki, E. Oset, and A. Ramos, Phys. Rev. **C61**, 055205 (2000);
K. Ikuta, M. Arima, and K. Masutani, Prog. Theor. Phys. **108**, 917 (2002);
J. Yamagata, H. Nagahiro, Y. Okumura, and S. Hirenzaki, Prog. Theor. Phys. **114**, 301 (2005) [Errata-*ibid* **114**, 905 (2005)];
J. Yamagata, H. Nagahiro, and S. Hirenzaki, Phys. Rev. **C74**, 014604 (2006).
 - [6] Q. Haider and L. C. Liu, Phys. Lett. **B172**, 257 (1986);
R. S. Hayano, S. Hirenzaki, and A. Gillitzer, Eur. Phys. J. A **6**, 99 (1999);
D. Jido, H. Nagahiro, and S. Hirenzaki, Phys. Rev. **C66**, 045202 (2002);
H. Nagahiro, D. Jido, and S. Hirenzaki, Phys. Rev. **C68**, 035205 (2003);
D. Jido, E. E. Kolomeitsev, H. Nagahiro, and S. Hirenzaki, Nucl. Phys. **A811**, 158 (2008).
 - [7] K. Suzuki *et al.*, Phys. Rev. Lett. **92**, 072302 (2004).
 - [8] H. Nagahiro, D. Jido, and S. Hirenzaki, Nucl. Phys. **A761**, 92 (2005).
 - [9] H. Nagahiro, D. Jido, and S. Hirenzaki, Phys. Rev. **C80**, 025205 (2009).
 - [10] H. Nagahiro and S. Hirenzaki, Phys. Rev. Lett. **94**, 232503 (2005).
 - [11] H. Nagahiro, M. Takizawa, and S. Hirenzaki, Phys. Rev. **C74**, 045203 (2006).
 - [12] D. Jido, H. Nagahiro and S. Hirenzaki, [arXiv:1109.0394 [nucl-th]].
 - [13] J. Yamagata-Sekihara, S. Hirenzaki, D. Cabrera, and M. J. Vicente-Vacas, Prog. Theor. Phys. **124**, 147 (2010).
 - [14] C. García-Recio, J. Nieves, and L. Tolos, Phys. Lett. **B690**, 369 (2010).
 - [15] A. Budzanowski *et al.*, Phys. Rev. **C79**, 012201(R) (2009).
 - [16] W. C. Parke and D. R. Lehman, Phys. Rev. **C29**, 2319 (1984).
 - [17] R. Ent *et al.*, Phys. Rev. Lett. **57**, 2367 (1986).
 - [18] R. Muto *et al.* [KEK-PS E325 Collaboration], Phys. Rev. Lett. **98**, 042501 (2007).
 - [19] T. Ishikawa *et al.*, Phys. Lett. **B608**, 215 (2005).
 - [20] E. C. Simpson and J. A. Tostevin, Phys. Rev. **C83**, 014605 (2011).
 - [21] P. Berthet *et al.*, Nucl. Phys. **A443**, 589 (1985).